Highly efficient surface enhanced Raman scattering using microstructured optical fibers with enhanced plasmonic interactions

Anna C. Peacock,[1,a)] Adrian Amezcua-Correa,[1] Jixin Yang,[2] Pier J. A. Sazio,[1] and Steven M. Howdle[2]
[1]*Optoelectronics Research Centre, University of Southampton, Southampton SO17 1BJ, United Kingdom*
[2]*School of Chemistry, University of Nottingham, Nottingham NG7 2RD, United Kingdom*

(Received 29 February 2008; accepted 17 March 2008; published online 10 April 2008)

Microstructured optical fibers (MOFs) represent a promising platform technology for fully integrated photonic-plasmonic devices. In this paper, we experimentally investigate the properties of two MOF templates impregnated with silver nanoparticles via a high pressure chemical deposition technique. By comparing fiber templates with different air filling fractions, we have quantified the importance of an increased field-particle overlap for improved surface enhanced Raman scattering sensitivity for the next generation of optical fiber sensors. © *2008 American Institute of Physics*. [DOI: 10.1063/1.2907506]

Optical fiber sensors offer a number of advantages over conventional electronic devices because they are compact, robust, flexible, and can stretch over kilometer lengths without the need for complicated electrical components near the active sensing region. Recently, there has been a great interest in fiberized devices which incorporate metallic thin films or nanoparticles due to the large electromagnetic fields generated via the excitation of surface plasmons.[1] The incorporation of metals into an optical fiber geometry combines photon transport with the active plasmonic region to yield completely integrated devices with unique excitation and detection geometries.

Since the demonstration of pure silica microstructured optical fibers[2] (MOFs), they have become an increasingly integral component in many areas of research and the current endeavors to incorporate functional materials into the air holes have led to the development of a range of complex in-fiber devices.[3–5] MOFs make exceptional three-dimensional templates for materials deposition as they are robust, temporally and mechanically stable, and the aperiodic or periodic arrangement of air holes can be tightly controlled during the fabrication process so that by choosing an appropriate structure, the distribution of the optical mode can be carefully engineered.[6] Using a high-pressure chemical deposition technique, we recently reported the deposition of silver nanoparticles into the voids of MOFs for use as surface enhanced Raman scattering (SERS) sensors.[7] Significantly, localized plasmonic excitation on nanoparticles does not suffer from the strict phase-matching requirements of plasmon waves on thin smooth films, simplifying the device design.[8] By exploiting the unique geometry of MOFs, where the light guided in the core can interact with the metal nanoparticles via the evanescent field, our fiberized sensors can provide enhanced propagation lengths and average over many particle sizes and spacings, thus offering increased sensitivity and reproducibility of the measured response.

In our previous work, we investigated the SERS properties of a MOF with a large core ($\sim 20\ \mu$m) relative to the visible wavelength of the excitation laser, so that the overlap between the core guided light and the nanoparticles in the cladding air holes was small. By measuring the SERS signals detected via two different excitation geometries, where in one instance the light was coupled into core guided modes (long interaction length but a small field-particle overlap) and in the other into cladding modes (large field-particle overlap but a short interaction length), we hypothesized that the SERS strength could be improved by optimizing the overlap between the core guided modes and the metal nanoparticles. With this motivation, in this paper, we now consider a small core ($\sim 1\ \mu$m) MOF design and compare its SERS efficiency with that of the original MOF. The effect of increased optical losses due to the incorporation of metals into the pure silica structures, as well as the significance of the enhanced field-particle overlap, is established by investigating different deposition profiles.

The functionalization of the fibers is performed using a high pressure chemical deposition technique described in detail in Ref. 7. Control over the silver deposition can be obtained by tuning the experimental parameters such as the temperature, precursor concentration, flow rate, and deposition time to yield a range of particle sizes from tens to hundreds of nanometers and profiles that vary from sparse nanoparticles to thin granular films. In our experiments, we compare two fiber templates: a large core fiber $\Lambda = 15\ \mu$m and $d = 11\ \mu$m, and a small core fiber $\Lambda = 1.4\ \mu$m and $d = 1\ \mu$m. Scanning electron microscope (SEM) micrographs of the templates are shown in Figs. 1(a) and 1(b). Although these fibers exhibit very different mass transport properties, we can nevertheless control the deposition conditions to obtain similar particle sizes in the two templates. This is illustrated in the remaining images of Fig. 1 where (c) and (d) show the fibers with small ~ 40 nm particle depositions and (e) and (f) show larger ~ 120 nm particle depositions.

Recently, a number of theoretical studies have been conducted to investigate the transmission properties of metal-dielectric MOF devices ranging from fibers with thin smooth coatings on the capillary walls to solid nanowire inclusions.[9–11] Unfortunately, similar modeling of our MOFs with metal nanoparticle inclusions is much more complicated owing to the size distribution of the metal particles and also the interparticle interactions which occur between neighboring particles with nanometer scale separations. However, some insight into how these fibers interact with the metal particles can simply be obtained by investigating the trans-

a)Electronic mail: acp@orc.soton.ac.uk.

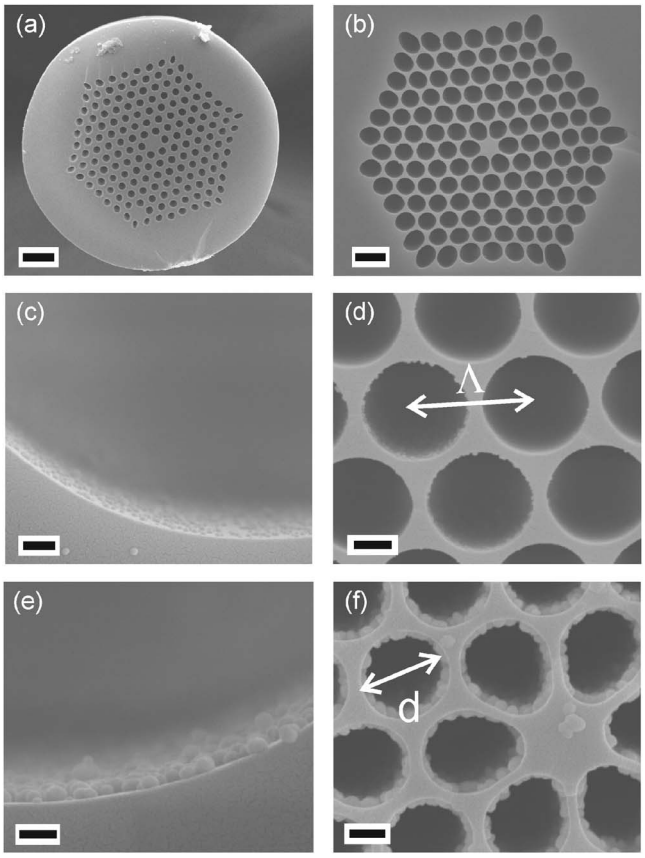

FIG. 1. SEM micrographs of MOFs with large (left) and small (right) cores. [(a) and (b)] Templates, scale bars 30 and 2 μm, respectively. [(c) and (d)] Small ~40 nm particle and [(e) and (f)] large ~120 nm particle depositions; scale bars 500 nm.

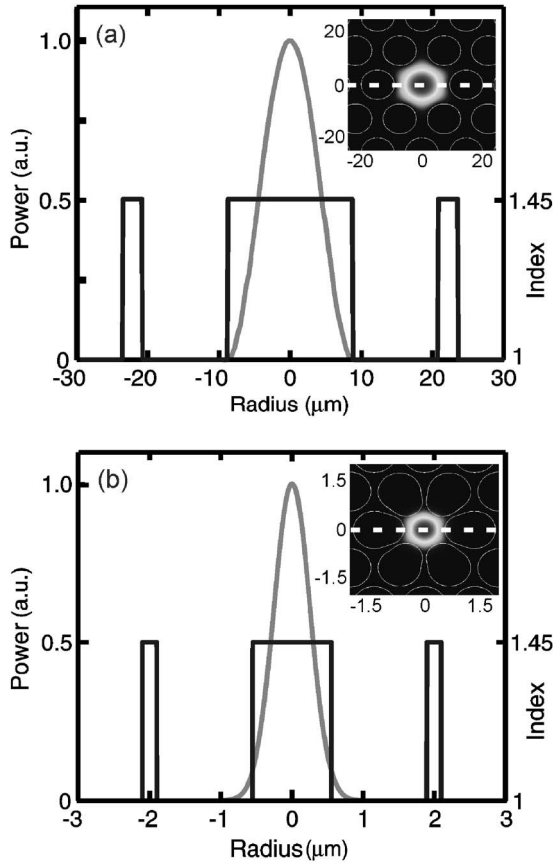

FIG. 2. Normalized power distribution of the fundamental guided modes, as a function of the radial position, for the (a) large and (b) small core fibers. Insets are 2D intensity profiles.

mission properties of the bare silica fiber templates. Using a full vectorial finite element method (FEM), we have calculated the guided modes of the two fibers for the visible excitation wavelength of 633 nm, which is used later in our SERS experiments. Figure 2 shows the fundamental guided modes for the two fibers where it is clear that there is significantly more of the field (>4000× the optical power) in the inner air holes of the small core fiber with which to interact with the silver nanoparticles. Furthermore, for this wavelength, both these fibers are multimodal possessing a number of core and cladding guided modes and in all cases the modes of the small core structure have orders of magnitude more power extending into the air holes.

The FEM calculations of the modes also enables us to determine the confinement loss of the fibers, which in both cases is negligible, so that the main contribution to the template losses is the material loss of ~4 dB/km. Clearly, the addition of metal into these fibers will dramatically increase the losses, both due to the imaginary component of the dielectric constant of silver and also due to the excitation of plasmon modes. Using the cut-back method, we have experimentally measured the losses for the fiber templates impregnated with silver at 633 nm. Owing to the high scattering losses of the large particle deposition fibers, to establish more comparative values for the two templates, we measured the losses for the small particle deposition fibers [Figs. 1(c) and 1(d)] and obtained ~0.6 dB/cm and ~1 dB/mm for the large and small core structures, respectively. This substantial increase in loss for the small core fiber is to be expected owing to the increased field-metal particle interaction. Nevertheless, by assuming a 3 dB device loss tolerance, realistic length scales for these silver fibers are in the range 0.3–5 cm which still provide a larger interaction area compared to a planar substrate where the area is determined solely by the spot size of the pump laser.

To compare the relative plasmonic properties of the two fiber templates, all four substrates [Figs. 1(c) to 1(f)] were tested for SERS activity using 4-aminothiophenol (4-ATP) as the target molecule. 4-ATP is a suitable molecule for investigating SERS due to its distinct Raman features, strong affinity for coinage-metal surfaces, and formation of self-assembled monolayers. All measurements were conducted using a conventional Renishaw Raman spectrometer with a 633 nm He–Ne excitation source focused using a 50× microscope objective to produce a spot size of approximately 2 μm in diameter with 3 mW of optical power. The fibers were sectioned in ~5 mm long samples and treated with a 0.5 mM solution of 4-ATP in ethanol using the capillary action to ensure that the thiol covers the entire silver surface area. After drying, the fibers are then flushed with pure ethanol to remove any excess thiol, thus, ensuring that there is only a thin, near monolayer of 4-ATP coating the silver.

The laser is focused into the fiber cores, so that most of the optical power is coupled into the low loss guided modes, and the scattered light is detected via the same input objective lens to collect the Raman photons that have recoupled into the high numerical aperture core. The measured SERS spectra of the two templates for both the small and large particle depositions are shown in Figs. 3(a) and 3(b). Control spectra taken on undoped fiber samples treated with 4-ATP in the same manner are overlayed on the spectra showing only

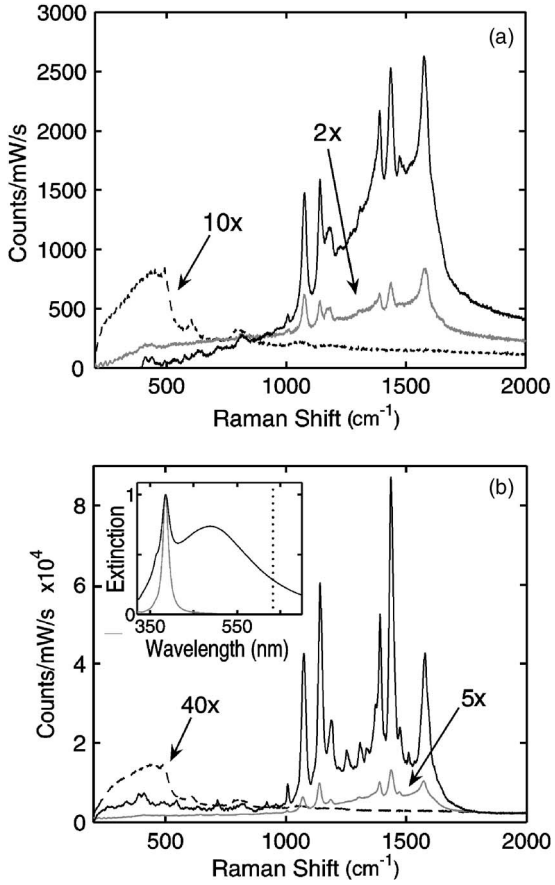

FIG. 3. SERS spectra for (a) large and (b) small core fibers. Gray lines are small particle depositions, black lines are large particle depositions, and dashed lines are control MOF with no silver filling. SERS spectra have been baseline shifted close to zero (Counts/mW/s). Inset: Mie scattering extinction curves for 40 nm (gray) and 120 nm (black) silver particles. Dotted vertical line is excitation wavelength.

the Raman spectrum of silica with no observable 4-ATP peaks. Although a strong signal is observed in all the silver impregnated fibers, with the main vibrational modes of the target molecule observed as reported in the literature,[12] there is a clear enhancement of the Raman signal in the small core structure. Comparing the relative SERS strengths, for the small particle deposition the signal in the small core structure is ~10× greater and increases to ~70× for the large particle deposition.

To aid with the interpretation of these results, we have calculated Mie scattering extinction curves for individual silver nanoparticles on a silica substrate, as shown in the inset of Fig. 3(b).[13] From these curves, we can attribute the modest SERS strengths for the small ~40 nm particle deposition fibers, in part, to the small overlap between the single plasmon resonance and the excitation wavelength, and the stronger signal for the larger particle deposition to the appearance of a second plasmon mode closer to the red wavelengths. It is thus likely that the increase in the relative SERS enhancements going from the small to large particles is partially due to the differences in the templates being emphasized by the stronger interaction between the plasmon modes and the excitation beam. In addition, although it is well known that interparticle interactions shift the plasmon resonances to even longer wavelengths, which would improve the overlap with our excitation wavelength,[1] as the small particle depositions are quite sparse [Fig. 1(c) and 1(d)] this effect will be greater for the larger particle depositions [Fig. 1(e) and 1(f)] further contributing to the increased relative enhancement. Owing to the unusual three-dimensional geometry of the MOF substrates and the particulate nature of the SERS surface, precise calculation of an enhancement factor following the conventional methods is nontrivial.[14] However, using the method and assumptions outlined in Ref. 7, we have estimated the enhancement factor of the small core substrate to be of the order 10^6 compared with 10^4 that we estimated for the large core fiber. This two orders of magnitude estimate in the enhancement for the small core fiber is reasonable if we trade off the increased optical power in the holes of the template modeling with the increased losses in the transmission measurements. Thus, these results highlight the significance of the increased overlap with the metal nanoparticles for improved plasmon excitation and enhanced SERS sensitivity.

We have compared two MOF templates with silver nanoparticle inclusions for use as plasmonic optical fiber sensors. By investigating the transmission properties of the fibers, both were shown to exhibit relatively low optical losses at visible wavelengths making it possible to excite many plasmon resonances along the fiber. Although the small core fiber structure demonstrated greater losses, the enhanced field-particle interaction resulted in orders of magnitude improved SERS sensitivity. The ability to control the losses and plasmon excitation simply via the choice of MOF design and the metal deposition profile opens up the potential for plasmonic fiber devices to be integrated with existing photonics infrastructures. The incorporation of the plasmon active region into the internal structure of a MOF provides a uniquely isolated and robust environment to investigate a range of photonic-plasmonic sensors.

The authors acknowledge EPSRC for support. A. Amezcua-Correa acknowledges the Mexican Council for Science and Technology for financial support. We also thank Mr. M. Guyler, Mr. R. Wilson, and Mr. P. Fields for their technical assistance. A. C. Peacock holds a RAEng fellowship and S. M. Howdle holds a RS Wolfson Research Merit Award.

[1] W. L. Barnes, A. Dereux, and T. W. Ebbesen, Nature (London) **424**, 824 (2003).
[2] J. C. Knight, Opt. Lett. **21**, 1547 (1996).
[3] C. Kerbage, A. Hale, A. Yablon, R. S. Windeler, and B. J. Eggleton, Appl. Phys. Lett. **79**, 3191 (2001).
[4] M. Fokine, L. E. Nilsson, A. Claesson, D. Berlemont, L. Kjellberg, L. Krummenacher, and W. Margulis, Opt. Lett. **27**, 1643 (2002).
[5] F. Benabid, J. C. Knight, G. Antonopoulos, and P. S. J. Russell, Science **298**, 399 (2002).
[6] J. C. Knight, Nature (London) **424**, 847 (2003).
[7] A. Amezcua-Correa, J. Yang, C. E. Finlayson, A. C. Peacock, J. R. Hayes, P. J. A. Sazio, J. J. Baumberg, and S. M. Howdle, Adv. Funct. Mater. **17**, 2024–2030 (2007).
[8] E. Kretschmann and Z. H. Raether, Z. Naturforsch. A **23**, 2135 (1968).
[9] B. T. Kuhlmey, K. Pathmanandavel, and R. C. McPhedran, Opt. Express **14**, 10851 (2006).
[10] A. Hassani and M. Skorobogatiy, Opt. Express **14**, 11616 (2006).
[11] C. G. Poulton, Opt. Lett. **32**, 1647 (2007).
[12] S. W. Han, S. J. Lee, and K. Kim, Langmuir **17**, 6981 (2001).
[13] C. F. Bohren, *Absorption and Scattering of Light by Small Particles* (Wiley, New York, 1940).
[14] Z.-Q. Tian, B. Ren, and D.-Y. Wu, J. Phys. Chem. B **106**, 9463 (2002).